A Mössbauer spectroscopy study of nanoscale Ge–Sn dispersions prepared by ball milling

P. Boolchand
Department of Electrical and Computer Engineering, University of Cincinnati, Cincinnati, Ohio 45221-0030

C. C. Koch
Department of Materials Science and Engineering, North Carolina State University, Raleigh, North Carolina 27695-7907

(Received 25 November 1991; accepted 23 June 1992)

Nanoscale mixtures of Ge/Sn, a nominally immiscible binary system, prepared by mechanical attrition have been studied by ^{119}Sn Mössbauer spectroscopy. The Mössbauer measurements in general reveal two sites for the Sn atoms, a tetragonal β–Sn site and another site designated as "A". The β–Sn integrated intensity decreases in magnitude with Ge concentration, $1 - x$, in $Ge_{1-x}Sn_x$ as the second A-site intensity increases. The isomer shift and the small/negligible quadrupole splitting of site A suggests it represents Sn in solid solution in the Ge lattice. This in turn represents a large (12–24 at. %) nonequilibrium solid solubility of Sn in Ge prepared by mechanical milling, compared to the equilibrium value of <1.0 at. %. Oxidation of the Sn was detected by Mössbauer spectroscopy at Sn-poor concentrations ($x \leq 0.10$) when the milling vial was not totally free of oxygen (i.e., milling in impure argon). This may be due to rapid oxidation of finely divided Sn film particles possessing a large surface-to-volume ratio at these compositions.

I. INTRODUCTION

The synthesis of materials by high energy ball milling—mechanical alloying or mechanical milling—offers exciting new possibilities for materials research.[1] Mechanical alloying (MA) is one of the few methods for producing a homogeneous mixture of two or more immiscible phases. Benjamin[2] first described the synthesis by MA of homogeneous mixtures of Fe–50 wt. % Cu, a system that exhibits limited solid solubility, as well as Cu–Pb alloys for which there is a liquid miscibility gap. Jang and Koch[3,4] have formed nanoscale dispersions of Ge particles in a Sn matrix by ball milling. After 32 h of milling in a shaker mill (Spex 8000) the average diameter of the Ge particles was ~10 nm and was essentially unchanged by additional milling. Calorimetric measurements indicated that the melting temperatures of Sn in these dispersions, even upon remelting after solidification, were depressed to values considerably below that, T_M°, of pure Sn. For a Ge volume fraction $V_{Ge} = 0.455$ melting was observed to begin as low as 36 °C below the equilibrium bulk melting temperature. It was concluded that the major contribution to the melting point depression, ΔT_M, comes from the nucleation of disorder/melting at the Ge/Sn interfaces. It was also found that as V_{Ge} was increased the measured enthalpy of melting per mass of total tin added, ΔH_M, decreased to levels well below that, ΔH_M°, of pure bulk Sn, and at $V_{Ge} > 0.81$ it was immeasurably small. This result was modeled by Turnbull *et al.*[5] by supposing that the Sn is distributed between an interfacial and bulk state. The interfacial state is one in which the Sn is assumed to be in a disordered, possibly amorphous state and coats the Ge particles uniformly to a constant thickness, d. The remaining "bulk" Sn is assumed to exhibit the normal enthalpy of fusion. The model accounts for the dependence of ΔH_M on V_{Ge} within experimental uncertainty. With the average size of Ge particles ~10 nm, d is estimated to be ~0.23 nm, i.e., of the order of the thickness of one Sn monolayer. Attempts to observe the Sn interfacial layer by TEM were inconclusive[4] although suggestions of amorphous halos were observed in electron diffraction patterns for samples with $V_{Ge} > 0.81$ near the position where the (101) Sn diffraction ring should appear.

^{119}Sn Mössbauer spectroscopy provides a sensitive probe of the nanostructure of these materials since Sn is the component of interest. In this paper we describe Mössbauer spectroscopy results on the $Ge_{1-x}Sn_x$ samples of Jang and Koch[4] and show that Sn exists in two distinct chemical states in these materials: bulk β–Sn and tetrahedral Sn incorporated into the Ge particle surfaces as a substitutional dopant. At low Sn concentrations, $x < 0.10$, a significant amount of Sn appears to be oxidized to Sn^{2+} and then to Sn^{4+}. These oxide peaks could be minimized/eliminated by milling under vacuum.

The consequences of these Mössbauer spectroscopy results on the interpretation of the nanostructure of the Ge/Sn composites prepared by ball milling will be discussed.

II. EXPERIMENTAL

Elemental powder mixtures of $Ge_{1-x}Sn_x$ at compositions $x = 1.0, 0.5, 0.3, 0.17, 0.15, 0.10$, and 0.05 were milled in a SPEX Industries 8000 Mixer/Mill following the procedures described earlier.[3,4] The milling container was a cylindrical tool steel vial and the milling media consisted of 440C martensitic stainless steel balls at a ball-to-powder mass ratio of 6:1. Mechanical milling was carried out at ambient temperature for 32 h during which the temperature of the vial rose to a maximum of 60 °C.

^{119}Sn Mössbauer spectra of powdered samples were taken at room temperature using a standard constant acceleration drive. A 10 mc quantity of ^{119}Sn in $CaSnO_3$ was used as a source of the 23.8 keV γ-rays which were detected with a thin-NaI scintillation counter. Spectra of the samples were analyzed in terms of the requisite number of singlets and doublets using our own software adapted to run on a 286 processor. Spectra of model compounds $BaSnO_3$ and β–Sn were recorded for comparison purposes. The drive was calibrated using the magnetic splitting in α–Fe and a ^{57}Co in Pd as a single line source of the 14.4 keV γ-rays.

III. RESULTS

Figures 1, 2, and 3 reproduce selected spectra of 32 h mechanically milled $Ge_{1-x}Sn_x$ mixtures at indicated Sn concentrations x. These were the samples used by Jang and Koch[4] in their previous study. For comparison we also show spectra of two reference compounds: β–Sn and $BaSnO_3$ in Fig. 1(a). Two types of line shapes can be observed in the spectra of the present samples; in the concentration range $1.0 < x < 0.15$ [see Figs. 1(a), 1(b), 1(c), and 2(a)] the spectra display a narrow feature centered at about 2 mm/s which can be deconvoluted largely in terms of two single lines labeled as A and β–Sn. At lower Sn concentrations $x \leqslant 0.19$ [see Figs. 2(b) and 2(c)] spectra in general are more complex; in addition to the sharp feature near 2.0 mm/s, we can observe weaker absorption near ~0 mm/s and near 3.5 mm/s. To deconvolute these complex line shapes we have included besides the two singlets labeled A and β–Sn, two additional doublets: the one centered near ~0 mm/s labeled as Sn^{4+} and the one centered near ~3.0 mm/s labeled as Sn^{2+}. In fitting the spectra we imposed only one constraint: the isomer-shift of the β–Sn singlet was kept fixed at 2.56 mm/s, the value characteristic of white Sn in the reference compound.

At a Sn concentration of $x = 0.10$ we studied the behavior of the line shape, particularly the doublets labeled Sn^{4+} and Sn^{2+}, as a function of milling atmosphere to test the assumption that the Sn^{2+} site was Sn in SnO and the Sn^{4+} site was Sn in SnO_2. In Fig. 3 the Mössbauer spectra of this composition are presented for three milling experiments in which the possibility of oxidation was minimized going from the case in Fig. 3(a) to that of Fig. 3(c). The powder (<45 μm diameter) prepared for the analysis shown in Fig. 3(a) was loaded in the milling vial under an atmosphere of argon (<1% oxygen). The powder for the sample measurement presented in Fig. 3(b) was prepared from elemental Sn and Ge powder evacuated overnight in the ball mill assembly using a cryopump and then backfilling with dry N_2 gas before ball milling. For the sample whose spectra are given in Fig. 3(c) the only difference in sample preparation from the sample of Fig. 3(b) was that we started with five large chips of elemental Sn and Ge instead of powders. Chips are easier to pump down largely because of a significantly smaller surface area. It is clear from Fig. 3(c) that this sample does not exhibit detectible evidence of the Sn^{4+} site in the spectra although small traces of Sn^{2+} are still resolvable. In Table I we compare the isomer-shift (δ) and quadrupole splitting (Δ) parameters of the various sites observed in the present ball-milled $Ge_{1-x}Sn_x$ samples with those of several reference compounds. The site intensity ratio, I_n/I, is plotted against composition in Fig. 4. This ratio is defined with $n = \beta$–Sn, A, Sn^{2+}, or Sn^{4+} sites with the total integrated intensity $I = I_{\beta\text{–Sn}} + I_A + I_{Sn^{2+}} + I_{Sn^{4+}}$ obtained from a deconvolution of the Mössbauer spectral line shape. This figure summarizes the composition dependence of the ratio of the site occupancies and shows the increase of the A site at the expense of the β–Sn site as Ge content increases. At the Ge-rich concentrations ($x \leqslant 0.15$) the oxide sites, Sn^{2+} and Sn^{4+}, appear but their intensity depends upon the processing. As oxygen contamination is reduced by milling in more oxygen-free environments ($3 \rightarrow 2 \rightarrow 1$ in Fig. 4), the intensity of the Sn^{4+} site disappears and that of the Sn^{2+} becomes very small. The tin oxide sites also disappear at higher Sn concentrations ($x > 0.15$). There appears to be a tendency for the finely dispersed Sn to oxidize readily, presumably because of the increased surface-to-volume ratio, in small clusters and films.

Figure 5 shows a plot of the site A isomer shift in the present mechanically milled $Ge_{1-x}Sn_x$ samples at several values of x and the results indicated a value of 1.90 (2) mm/s (Table I). Site A is characterized with no measured quadrupole splitting. The observed linewidth for the β–Sn site and site A (Figs. 1 and 2) were kept the same and these typically refined to a value of about 0.9 mm/s. This indicates that the quadrupole splitting of site A, if finite, is actually <0.1 mm/s. The small size

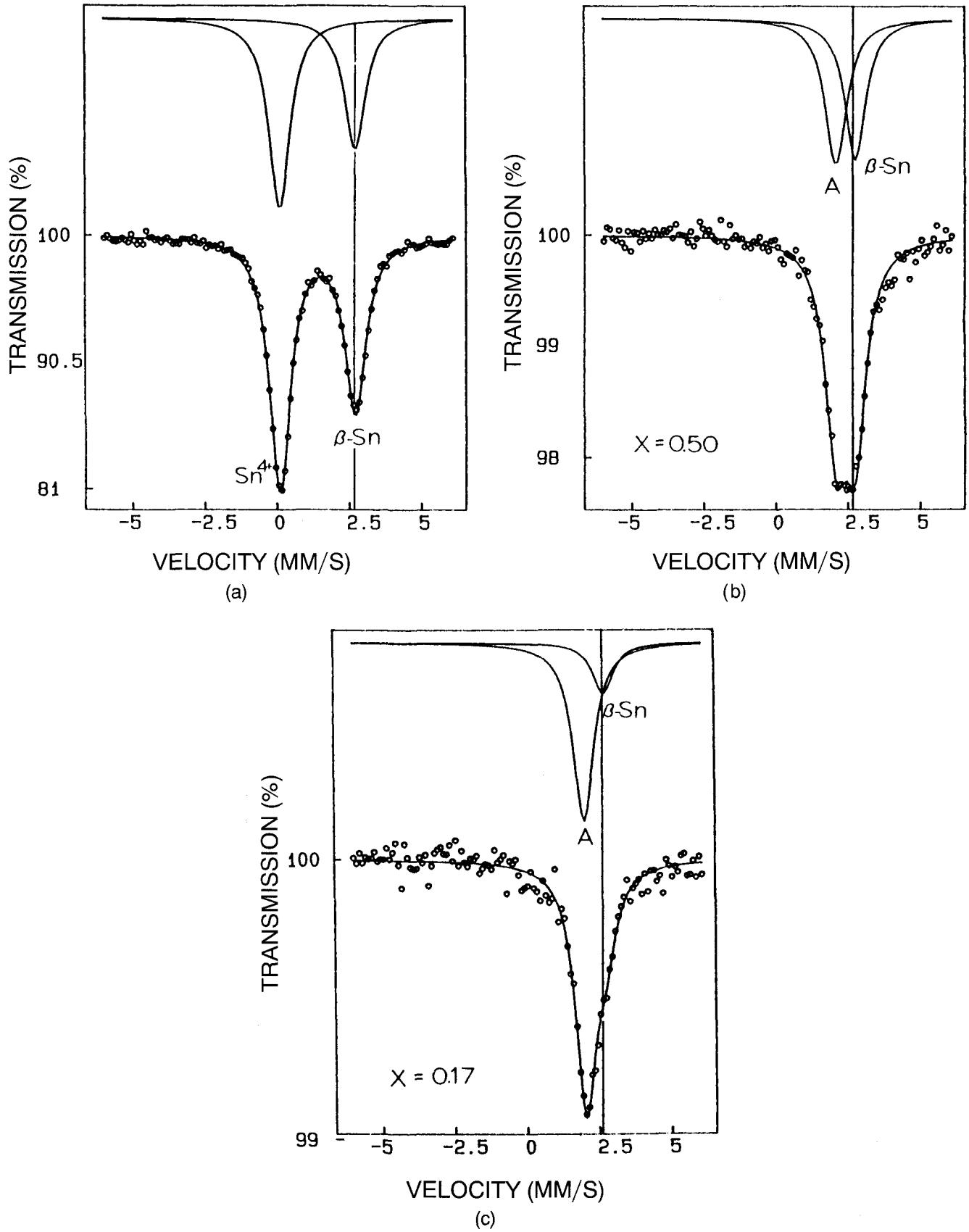

FIG. 1. Mössbauer spectra for (a) reference compounds β–Sn and $BaSnO_3$, (b) $Ge_{1-x}Sn_x$ for $x = 0.50$ milled 32 h, and (c) $Ge_{1-x}Sn_x$ for $x = 0.17$ milled 32 h.

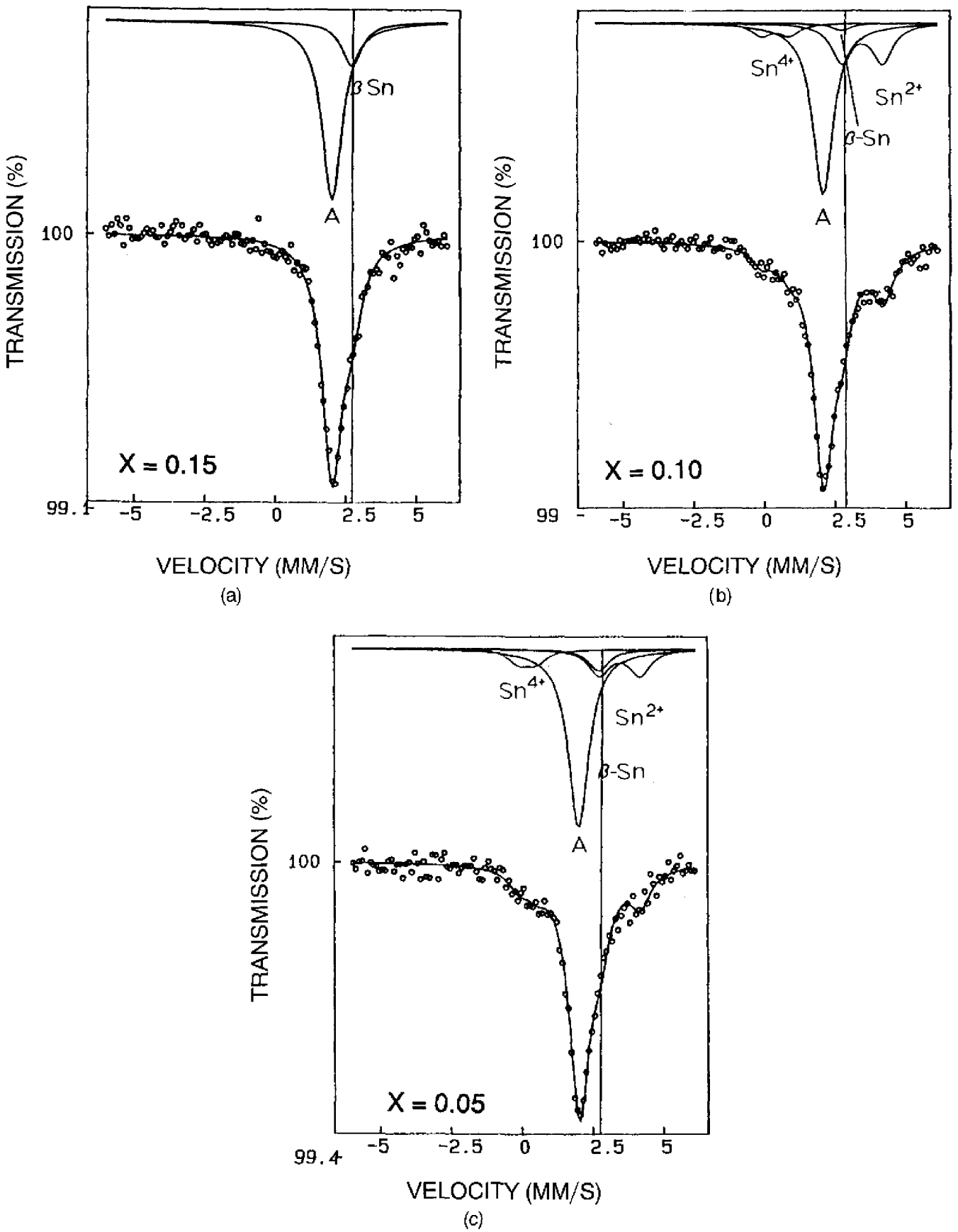

FIG. 2. Mössbauer spectra for $Ge_{1-x}Sn_x$ milled 32 h for (a) $x = 0.15$, (b) $x = 0.10$, and (c) $x = 0.05$.

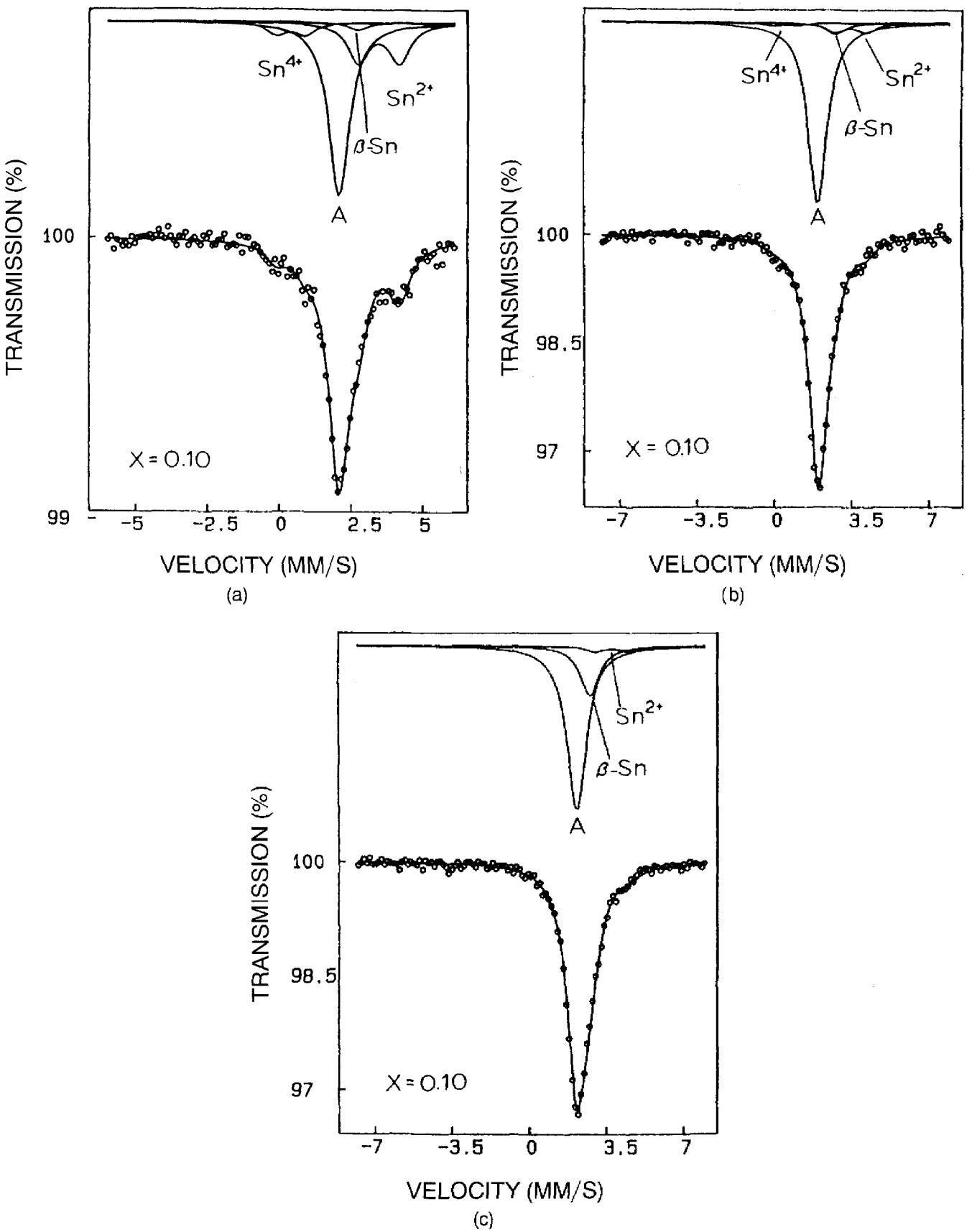

FIG. 3. Mössbauer spectra of $Ge_{1-x}Sn_x$ milled 32 h for $x = 0.10$. Oxygen contamination decreases from (a) (powder milled in argon) (b) (powder milled in dry N_2 after evacuating the vial) to (c) (chips of Ge, Sn milled in dry N_2 after evacuating the vial).

TABLE I. Mössbauer data: Isomer shift (δ) and quadrupole splitting (Δ) parameters for Sn sites in $Ge_{1-x}Sn_x$ and related structures.

Sample	δ[a] (mm/s)	Δ (mm/s)	References
$Ge_{1-x}Sn_x$:			
Site A	1.90(4)	~0	This work
Sn^{2+}	3.30(10)	1.43(10)	This work
Sn^{4+}	~0	~0.9	This work
β–Sn	2.57[b]	0	This work
α–Sn	2.01(4)	0	6, 7
β–Sn	2.56(2)	0	6
c-SnO (red)	2.60	2.20	6
c-SnO (black)	2.71	1.45	6
$c\text{-}SnO_{2-y}O$	~0.5		
$a\text{-}Sn_xCu_{1-x}$	2.75	...	8, 9
Sn in c-Ge	1.90	...	7, 10

[a]Relative to $BaSnO_3$ at 300 K.
[b]Kept fixed in lineshape analysis of ball-milled $Ge_{1-x}Sn_x$ samples.

of the quadrupole splittings suggests a rather symmetric environment for site A such as a cubic or tetrahedral coordination of the Sn atom.

IV. DISCUSSION

A. Site assignments

The most important result of the Mössbauer study of the milled $Ge_{1-x}Sn_x$ powder is the identification of the A site of Sn. The results of Table I strongly suggest that this site be identified with Sn tetrahedrally coordinated to four Ge nearest-neighbors, as illustrated in Fig. 5(a). The isomer-shift of A-site coincides with that of Sn substitutional in c-Ge.[7,10] Furthermore, the absence of any measurable quadrupole splitting is in harmony with the proposed tetrahedral symmetry of the A-site largely because such a local symmetry ensures that the valence contribution of the Electric Field Gradient vanishes. We note that the isomer-shift of A-site is distinctly different from the shift of a Sn-site in amorphous Sn[8,9] or α–Sn.[6,7] On the other hand, the Sn^{2+} and Sn^{4+} sites observed

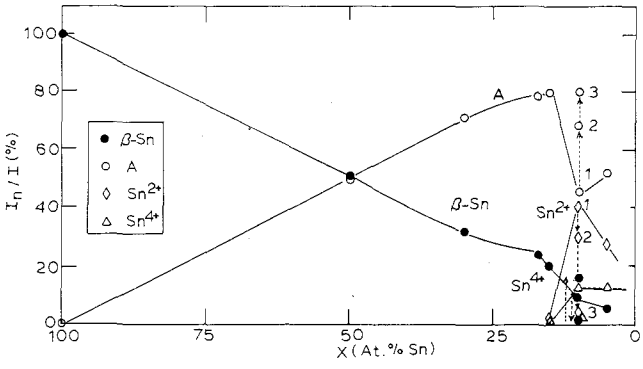

FIG. 4. Mössbauer site intensity ratio I_n/I as a function of composition x (at. % Sn).

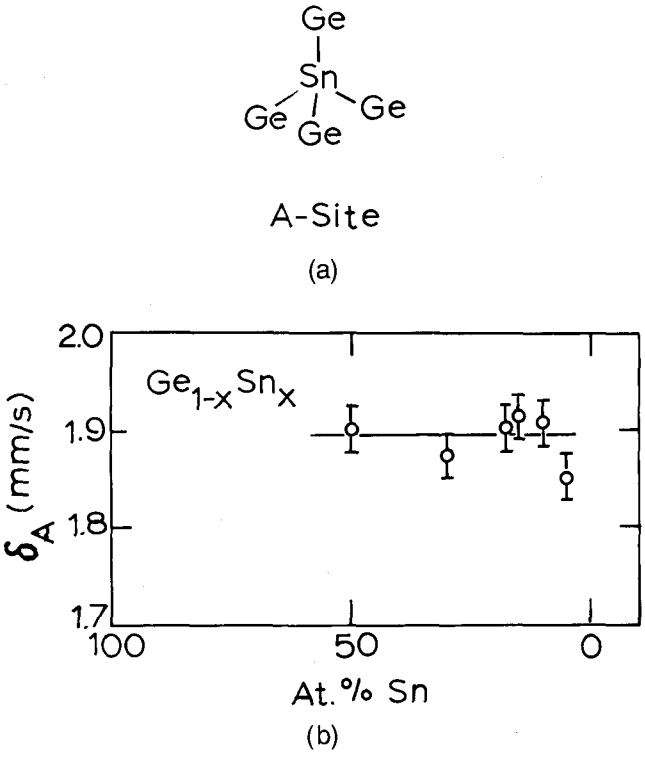

FIG. 5. (a) Schematic illustration of Sn coordinated to 4 Ge nearest-neighbors and (b) site A isomer shift δ_A in $Ge_{1-x}Sn$ as a function of composition x (at. % Sn).

in the milled $Ge_{1-x}Sn_x$ samples are clearly oxygen-associated, as demonstrated by the results of Fig. 3. It is quite likely that the environment of Sn for the Sn^{2+} site is probably similar to that of the black form of SnO while that for the Sn^{4+} site is similar to that of nonstoichiometric SnO_2. SnO and SnO_2 usually display some oxygen astoichiometry. The differences in δ and Δ parameters of the Sn^{2+} and Sn^{4+} sites between the ball-milled samples and those in c-SnO and $c\text{-}SnO_2$ may reflect the formation of nonstoichiometric oxides in the ball-milled samples.

B. Nanoscale structure of milled $Ge_{1-x}Sn_x$

In rationalizing the melting point depression, ΔT_M, and decrease in the enthalpy of fusion, ΔH_M, it was assumed[4,5] that the interfacial component consisted of an amorphous film of Sn atoms (approximately one monolayer) coating the Ge particles. However, the present Mössbauer effect results suggest that the interfacial Sn component is most probably associated with Sn atoms in substitutional solid solution in the surface of the Ge particles. This conclusion then would separate the effects of Ge concentration on the depression of T_M° for Sn and the enthalpy of fusion, ΔH_M. The melting point depression for Sn would continue to be rationalized[4] as the consequence of the nucleation of melting at the Ge/Sn interfaces. However, the decrease of ΔH_M, and

its disappearance for $V_{Ge} \geq 0.81$, must now be explained by the Sn component which does not contribute to ΔH_M originating as Sn in solid solution in Ge. The calorimetry of Jang and Koch[4] indicated that $\Delta H_M = 0$ for $V_{Ge} \geq 0.81$, suggesting that no bulk β–Sn was present in this range of compositions. This is consistent with the Mössbauer effect results shown in Fig. 3(a) for $x = 0.10$. A negligible peak for β–Sn is obtained by deconvolution of the data which indicates that the Sn is tied up in solution in Ge (site A) and/or as oxides (SnO and SnO_2). The sample of Fig. 3(a) was the same one used for the calorimetry. Presumably, the sample of Fig. 3(c), which exhibits a finite contribution from β–Sn, would also give a measurable value for ΔH_M.

C. Solubility of Sn in c-Ge in milled $Ge_{1-x}Sn_x$

The Ge–Sn equilibrium diagram exhibits little solubility of Ge in Sn and very limited solubility for Sn in Ge.[11] The maximum solubility is about 1.1 at.% Sn at 400 °C, i.e., where Sn is liquid, about 1.0 at.% Sn at the eutectic temperature (231.1 °C) and less than 0.5 at.% at room temperature. However, the Mössbauer results of the Ge–Sn powders milled 32 h suggest substantially greater solubilities than the equilibrium values. Specifically, if we assume that the Debye–Waller factor of the four Sn species observed in the $Ge_{1-x}Sn_x$ samples are the same, then the site intensity ratios (I_n/I) of Fig. 4 become a quantitative measure of site concentrations. We note that at an average composition of 15 at.% Sn, about 80% of the Sn atoms are actually incorporated in the Ge lattice (the A site), giving a nonequilibrium solid solubility of Sn in Ge of ~12 at.% Sn. Similarly, at an average composition of 50 at.% Sn, ~48% of the Sn atoms are in the Ge lattice, suggesting a solubility of 24 at.% Sn in Ge. The apparent composition dependence of a nonequilibrium solid solubility of Sn in Ge was observed previously in rapid solidification (splat cooling) experiments by Kuzmin and Nikitina.[9] The average compositions and apparent solubilities are listed in Table II.

The nonequilibrium nanoscale dispersions produced by ball milling clearly show a significantly higher solid solubility for Sn in Ge than the reported rapid solidification study. Ivanov[12] has recently reported a large nonequilibrium solubility of Hg in Cu of about 70 at.% for Cu–Hg alloys prepared by ball milling, compared to equilibrium solubilities of less than 1 at.%. No details of the microstructure were given. The nanocrystalline structure produced during ball milling for long times may be responsible for the large enhancement in solid solubilities. Enhanced solubilities have been observed in nanocrystalline materials produced by the gas condensation method. For example, Birringer *et al.*[13] have observed the solubility of Bi (at 373 K) in nanocrystalline Cu (average grain size, 10 nm) of 4 at.% compared to the equilibrium value of $<10^{-4}$ at.%. It is assumed that the solute atoms must be segregated to the grain boundary region, which for nanocrystalline grain sizes can amount to significant fractions of the total numbers of atoms in the material—up to 50% or more.

TABLE II. Nonequilibrium solid solubilities Ge (Sn).[9]

Average composition	Apparent solubility
25 at.% Sn	1 at.% Sn
30 at.% Sn	6 at.% Sn
50 at.% Sn	12 at.% Sn

D. Oxidation of nanoscale sized Sn particles

The results of Fig. 4 clearly demonstrate that oxidation of the Sn particles is observed only at low Sn concentration ($x \leq 0.15$). Enhanced diffusion paths may result from the fine distribution of Sn films surrounding the ~ equiaxed Ge nanocrystals. It should be emphasized that the *powder* dimensions are of the order of 0.5 to 1.0 μm and the nanoscale structure of Ge and Sn is contained in the powder particles. However, the Ge/Sn interfaces may provide an easy path for oxygen diffusion and coupled with the film-like Sn morphology at the Ge-rich compositions Sn oxidation can occur more readily since the thickness of the Sn films between the Ge/Sn interfaces decreases with increasing Ge concentration. In this context we note that the local Sn–O coordinations formed qualitatively bear a similarity to those known in crystalline SnO and SnO_2, as revealed by the Mössbauer parameters of Table I.

V. SUMMARY AND CONCLUSIONS

Mössbauer spectroscopy measurements reveal two major sites for the Sn atoms in nanoscale Ge/Sn dispersions prepared by ball milling. These are tetragonal β–Sn and another site termed the A site. The β–Sn site-intensity ratio decreases at the expense of the A site intensity ratio with increasing Ge concentration in the $Ge_{1-x}Sn_x$ samples. The isomer-shift of the A site and the small/negligible quadrupole splitting of this site strongly suggest that it represents Sn in solid solution in the Ge lattice. This conclusion is in contrast to the previous assumption that Sn atoms not contributing to the measured enthalpy of fusion in milled Ge/Sn dispersions were in the form of a disordered/amorphous film surrounding the Ge particles. The Mössbauer results point to a large (12–24 at.%) nonequilibrium solid solubility of Sn in Ge after mechanical milling. The fine nanocrystalline structure (Ge particle diameters ~10 nm) is presumably responsible for the enhanced solubilities.

Oxidation of Sn was observed only at Ge-rich compositions ($x \leq 0.15$) when the atmosphere of the milling vial was not completely free of oxygen (i.e., impure argon). This may be due to the finely divided morphology of the Sn films at these compositions.

NOTE ADDED IN PROOF

J. K. D. S. Jayanetti, S. M. Heald, and Z. Tau, of Brookhaven National Laboratory, have recently carried out EXAFS measurements on Ge/Sn milled powders which support our Mössbauer results regarding the surface alloying of Sn in Ge. Their paper is submitted to Phys. Rev. B.

ACKNOWLEDGMENTS

The authors' research was supported by the National Science Foundation under Grant No. DMR-89-02836 (P.B.) and Grant No. DMR-8620394 (C.C.K.). The authors wish to thank the following for assistance with the experimental work: A. Bhutiani, R. Burrows, Ray Enzweiler, and Mark Soper (University of Cincinnati) and Robert Leonard (North Carolina State University).

REFERENCES

1. C. C. Koch, "Mechanical Milling and Alloying," Chapter 5 in Volume 15: Processing of Metals and Alloys, edited by R. W. Cahn, from *Materials Science and Technology, a Comprehensive Treatment,* edited by R. W. Cahn, P. Haasen, and E. J. Kramer (VCH, Weinheim, Germany, 1991).
2. J. S. Benjamin, Sci. Am. **234**, 40 (1976).
3. C. C. Koch, J. S. C. Jang, and S. S. Gross, J. Mater. Res. **4**, 557 (1989).
4. J. S. C. Jang and C. C. Koch, J. Mater. Res. **5**, 325 (1990).
5. D. Turnbull, J. S. C. Jang, and C. C. Koch, J. Mater. Res. **5**, 1731 (1990).
6. N. N. Greenwood and T. C. Gibb, *Mössbauer Spectroscopy* (Chapman and Hall Ltd., London, 1971).
7. G. Weyer, A. Nylandsted-Larsen, B. I. Deutch, J. V. Andersen, and E. Antoncik, Hyp. Int. **1**, 93 (1975).
8. J. Bolz and F. Pobell, Z. Physik **B20**, 95 (1975).
9. R. N. Kuzmin and S. V. Nikitina, Sov. Phys. Solid State **13**, 3151 (1972).
10. M. Taniwaki, M. Uneta, K. Kasaya, and M. Maeda, J. Non Cryst. Solids **117–118** (pt. 1), 363 (1990).
11. R. W. Olesinski and G. J. Abbaschian, Bulletin of Alloy Phase Diagrams **5**, 265 (1984).
12. E. Ivanov, International Symposium on Mechanical Alloying (ISMA), May 7–10, 1991, Kyoto, Japan, Mater. Sci. Forum (Trans. Tech. Pub., Switzerland, 1992), Vol. 88–90, p. 475.
13. R. Birringer, H. Hahn, H. Höfler, J. Karch, and H. Gleiter, Defect and Diffusion Forum **59**, 17 (1988).